JOURNAL OF SOLID STATE CHEMISTRY 139, 176–184 (1998)
ARTICLE NO. SC987829

Polaronic Conduction in $La_{2-x}Sr_xCoO_4$ ($0.25 \leq x \leq 1.10$) below Room Temperature

E. Iguchi, H. Nakatsugawa, and K. Futakuchi

Materials Science, Department of Mechanical Engineering and Materials Science, Faculty of Engineering, Yokohama National University, Tokiwadai, Hodogaya-Ku, Yokohama, 240-8501 Japan

Received October 9, 1997; in revised form March 17, 1998; accepted March 18, 1998

Electrical transports in the $La_{2-x}Sr_xCoO_4$ system ($0.25 \leq x \leq 1.10$) below room temperature were investigated by bulk conductivities and dielectric properties in polycrystalline specimens. The bulk conductivities were obtained by complex-plane impedance analyses. For $x \leq 1.00$, every specimen contains a dielectric relaxation process which yields the electron transfer integral, J. The J values in these specimens meet the requirements for hopping conduction of nonadiabatic small polarons. The relation between the energy required for the conduction and the energy responsible for the dielectric relaxation also ensures the nonadiabatic polaronic conduction. The peculiarity due to the ordered state shows up in the conduction at $x=0.50$. For $x \geq 1.00$, every specimen involves a transition from the high temperature conduction process to the low temperature one. The transition point is near the Curie temperature, which indicates the strong correlation between spin alignment and carriers and also the change of the nature of carriers at the Curie point.

INTRODUCTION

The discovery of high T_C cuprate superconductors with layered structures like the K_2NiF_4-type, a two-dimensional analog of the perovskite-type (1), have rekindled interest and underscored the importance of the strongly correlated electron systems not only from the scientific point of view but also from an application viewpoint. Emin tried a theoretical interpretation on the high T_C superconductivities in terms of large bipolarons (2–4). If in fact polaronic conduction plays an important role in electrical transports in strongly correlated oxides, then it is of great importance to investigate whether the in-plane electronic transport of large bipolarons is also plausible in noncuprate oxides with layered structures or whether the exceptional conduction occurs only in the cuprate layered oxides, which become superconductors at low temperatures. To this end, the present work employs the $La_{2-x}Sr_xCoO_4$ system as an illustrative example because this system is in a homologous series with the K_2NiF_4 structures (5–9) and there are no experiments on the electrical transports at rather low temperatures. The traditional interpretation based on the experiments at high temperatures (around 500 K) holds that the conduction is due to hopping processes of adiabatic small polarons (10–12). However, this interpretation requires more direct support.

The electronic transport properties of large and small polarons are qualitatively different from one another. Large polarons move with significant mobilities that fall with increasing temperature. By contrast, small polarons move with very low mobilities that increase with increasing temperature (13). Large polarons are rather itinerant and the dc conductivity has a form of $\sigma \propto \exp(-E/k_BT)$ where E is the energy for generating carriers and k_B is Boltzmann's constant. Small polarons are rather localized because they are formed when the short-range components of the electron-phonon interaction predominate. The hopping process has a high probability of involving a dielectric relaxation as the carriers are excited from the potential wells associated with their self-trapping (14–21). There are two sorts of small polarons, i.e., an adiabatic small polaron and a nonadiabatic small polaron (13). These small polarons have the characteristic temperature dependencies of conductivities, i.e., $\sigma \cdot T^\gamma \propto \exp(-E/k_BT)$, $\gamma = 1$ for the adiabatic case and 3/2 for the nonadiabatic case, where the dominant component of E is the hopping energy of small polarons, W_H. However, it is practically difficult to identify the type of small polarons using only temperature dependence of conductivities because the conductivities subject to the adiabatic polaronic condition satisfy the nonadiabatic temperature dependence as well. A hopping process of nonadiabatic small polarons must meet several requirements for the electron transfer integral between neighboring hopping sites, which are then to be the criteria for judging whether the nonadiabatic hopping conduction is predominant (13, 22–25).

The crystallographic structures and magnetic properties of the $La_{2-x}Sr_xCoO_4$ system are well investigated (5, 6, 9–12, 26–32). As for the electrical transports, however, there are only a limited number of studies treating the conduction

0022-4596/98 $25.00

behavior at rather high temperatures (10–12, 32). Le Coustumer *et al.* (10) and Matsuura *et al.* (11, 12) interpreted their results in terms of hopping adiabatic small polarons. Matsuura *et al.* suggested that the electronic structure of Co-3*d* levels split by the partial removal of the electronic degeneracy played an important role in the electronic transports in this system; their argument was based on a Mott-Hubbard insulator (11, 12). In light of the ZSA theory (33), however, the optical study on $LaSrMO_4$ (M = Cr, Mn, Fe, and Co) by Morimoto *et al.* yielded the charge transfer (CT) gap of 1 eV in $LaSrCoO_4$ (34). The energy gap between the split Co-3*d* levels is remarkably narrow compared with CT band gaps (6, 7, 35). The positive thermopower in this system indicates that the doped holes are the majority carriers (11, 12).

Though the conduction experiments on the $La_{2-x}Sr_xCoO_4$ system at rather high temperatures obtain the results favoring of the polaronic scenario, more direct evidence is required. Dielectric properties can provide very important information regarding small polaron dynamics, as shown in our previous reports (17–21). The "conduction" described here means the bulk conduction and does not include the boundary conduction. The single crystal approach is the most straightforward and the most usual. Matsuura *et al.* (11) and Morimoto *et al.* (32, 34) succeeded in preparation of single crystals of this system, and their results should be referred to very carefully. Even if polycrystalline specimens are employed, however, the complex-plane impedance analysis can distinguish the bulk conduction from others (36–38). The impedance analysis would then provide very important results, leading directly to the real feature of the electrical transports in this system.

Matsuura *et al.* (11) reported activation energies less than 0.5 eV required for conduction in the $La_{2-x}Sr_xCoO_4$ system at high temperatures around 500 K. Morimoto *et al.* (34) obtained a similar result. Electronic conduction with such a low activation energy takes place even below room temperature. Furthermore, a dielectric relaxation due to a hopping process of small polarons with such a low activation energy also shows up generally below room temperature at the applied frequencies of alternating fields less than 1 MHz (17–21).

From this point of view, using a combination of the bulk conductivity and dielectric measurements, the present work will investigate the transport properties in the $La_{2-x}Sr_xCoO_4$ system ($0.25 \leq x \leq 1.10$) below room temperature.

EXPERIMENTS

The $La_{2-x}Sr_xCoO_4$ specimens (x = 0.25, 0.50, 0.75, 1.00, 1.05, and 1.1) were prepared by the conventional solid state synthesis technique. La_2O_3, Co_3O_4, and $SrCO_3$ (4N) powders were used. First, the mixed powders were calcined in air at 1200°C for one day. After being ground and mixed well, this heating process was repeated. Then the powders were pressed into pellets and sintered in pure flowing nitrogen at 1350°C for one day for $x \leq 0.50$ and in pure flowing oxygen for two days for $x \geq 0.75$. Cu$K\alpha$ X-ray diffraction of every specimen showed a single phase. The diffraction pattern of the orthorhombic La_2CoO_4 agrees well with the data in JCPDS (Code 34–1081). There are no JCPDS codes for other specimens, but the lattice parameters calculated using the X-ray diffraction data are nearly equal to those of Matsuura *et al.* (11). The densities of the sintered specimens were about 90% of the theoretical values, which were calculated using the lattice constants obtained in X-ray measurements.

Capacitance and impedance were obtained as functions of temperature by the four terminal pair ac impedance measurement method, using an HP 4284A precision LCR meter with a frequency range of 30 Hz to 1 MHz. The measured values of capacitance and impedance were corrected by calibrating capacitance and resistance of leads to zero. Flat surfaces of the specimens were coated with an In–Ga alloy in 7:3 ratio by a rubbing technique for an electrode. Evaporated gold was also used for the electrode but no significant difference was found in experimental results. A Maxwell-Wagner type polarization due to heterogeneity in a specimen was excluded because there is no significant difference in frequency dependency of dielectric constant at 200 K even if the thickness of the specimen is reduced to half.

A Keithley 619 resistance bridge, an Advantest TR 6871 digital multimeter, and an Advantest R 6161 power supply were used for dc conductivity measurements by the four probe method. The copper constantan pre calibrated at 4.2, 77, and 273 K was used for the temperature measurements.

Following the detailed account of the theoretical treatment (36–38), the complex-plane impedance analyses were carried out. Usually, in polycrystalline ceramics, three independent semicircular arcs show up in the impedance plots where the real part (Z') of the total impedance is plotted against the imaginary part (Z'') as a parametric function of frequency f, i.e., the highest-frequency arc corresponding to the bulk conduction, the intermediate one due to the conduction across the grain boundary, and the lowest-frequency arc coming from the transport across the electrode-specimen interface. The resistance values of the circuit elements are obtained from the real axis intercepts. Figure 1 depicts complex-plane impedance plots at several temperatures for $x = 0.25$. The solid line curves were determined by the least-mean-square analyses. Since the lowest-frequency arc was not observed in every specimen throughout the frequency range employed in the present work, there must be no electrode polarization in the electrode-specimen interfaces. The highest-resistance value of the intermediate arc is the total resistance in grains and boundaries.

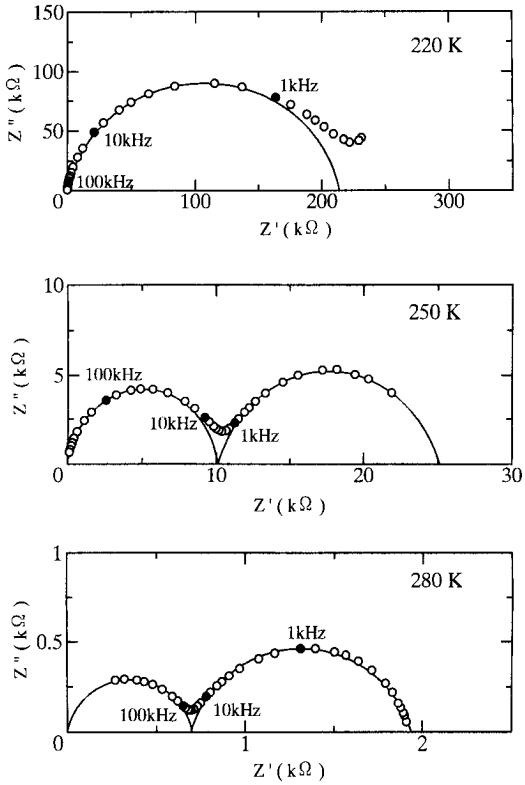

FIG. 1. The complex-plane impedance plots at 220, 250, and 280 K for $x = 0.25$. Z' and Z'' are the real and imaginary parts of the total impedance at each applied frequency.

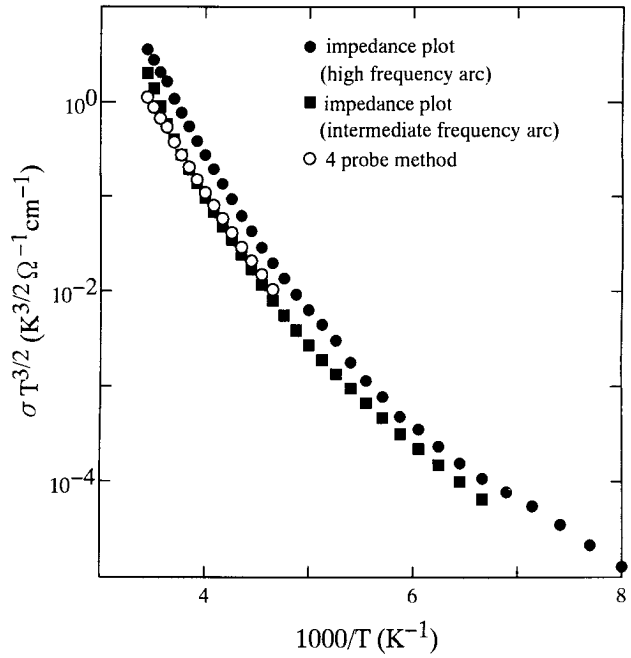

FIG. 2. Three Arrhenius relations of $\sigma \cdot T^{3/2}$ vs $1/T$ for $x = 1.00$, employing the bulk conductivity obtained from the real axis intercept of the highest frequency arc in the impedance analyses, the conductivity estimated from the highest resistance of the intermediate semicircular arc, and the dc conductivity obtained by the four-probe method.

Figure 2 plots Arrhenius relations of $\sigma \cdot T^{3/2}$ and $1/T$ for $LaSrCoO_4$ ($x = 1.00$), employing three sorts of conductivity, i.e., the conductivity obtained from the highest resistance of the highest-frequency arc (i.e., the bulk conductivity), the one estimated from the highest resistance of the intermediate arc, and the dc conductivity measured by the four-probe method. Since the plots of the dc conductivities and the ones obtained from the highest resistances of the intermediate arcs overlap one another, the four-probe method measures the total resistance in grains and boundaries.

Employing the bulk conductivities, Fig. 3a shows the plots of the Arrhenius relations of $\sigma \cdot T^{3/2}$ and $1/T$ for $x = 0.25$, 0.50, 0.75, and 1.00 at $T > 220$ K; similar relations are plotted in Fig. 3b for $x = 1.00$, 1.05, and 1.10 at $T > 70$ K. The impedance analysis on the specimen of $x = 0.25$ was impractical below 190 K because of the high resistance. The inset in Fig. 3a illustrates the relationship between σ and T for $x = 0.25$. At 200 K, $\sigma \cong 2 \times 10^{-7}\,\Omega^{-1}\,cm^{-1}$. In case of such a high resistivity, every impedance plot at $f \leq 1$ MHz is close to the origin and the highest-frequency arc is barely obtained by the aid of the least-mean-square analysis. At lower temperatures, the resistivity increases more and frequencies lower than the minimum in the present experiment are required. At $T > 315$ K, conversely, frequencies higher than the maximum in the present experiment, i.e., 1 MHz, are necessary. A similar situation holds in every specimen but the upper and lowest temperatures vary from specimen to specimen.

At $T > 220$ K in Fig. 3a, there is a linear portion in every specimen for $x \leq 1.00$. The activation energies are 0.56, 0.68, 0.43, and 0.38 eV for $x = 0.25$, 0.50, 0.75, and 1.00, respectively. As described in the Introduction, these plots also satisfy the Arrhenius relations of $\sigma \cdot T$ and $1/T$ with activation energies slightly lower than those obtained in Fig. 3a, approximately by 0.02 eV. The energies in nonadiabatic Arrhenius plots are nearly equal to the results of Matsuura *et al.* (11) and Morimoto *et al.* (32) but naturally a little higher because they employed adiabatic Arrhenius plots. As shown in Fig. 3b, every specimen has two thermally activated conduction processes for $x \geq 1.00$. The deviation from the high temperature conduction process with decreasing temperature occurs at ~ 200, ~ 195, and ~ 190 K for $x = 1.00$, 1.05, and 1.10, respectively. It is very interesting that these temperatures are very near the Curie point, which decreases from ~ 220 K to ~ 200 K as x increases from 1.0 to 1.1, although Curie temperatures are somewhat high (31). The activation energies required for the high-temperature processes are 0.38, 0.20, and 0.16 eV, and those for the low-temperature ones are 0.13, 0.083, and 0.079 eV for $x = 1.00$, 1.05, and 1.10.

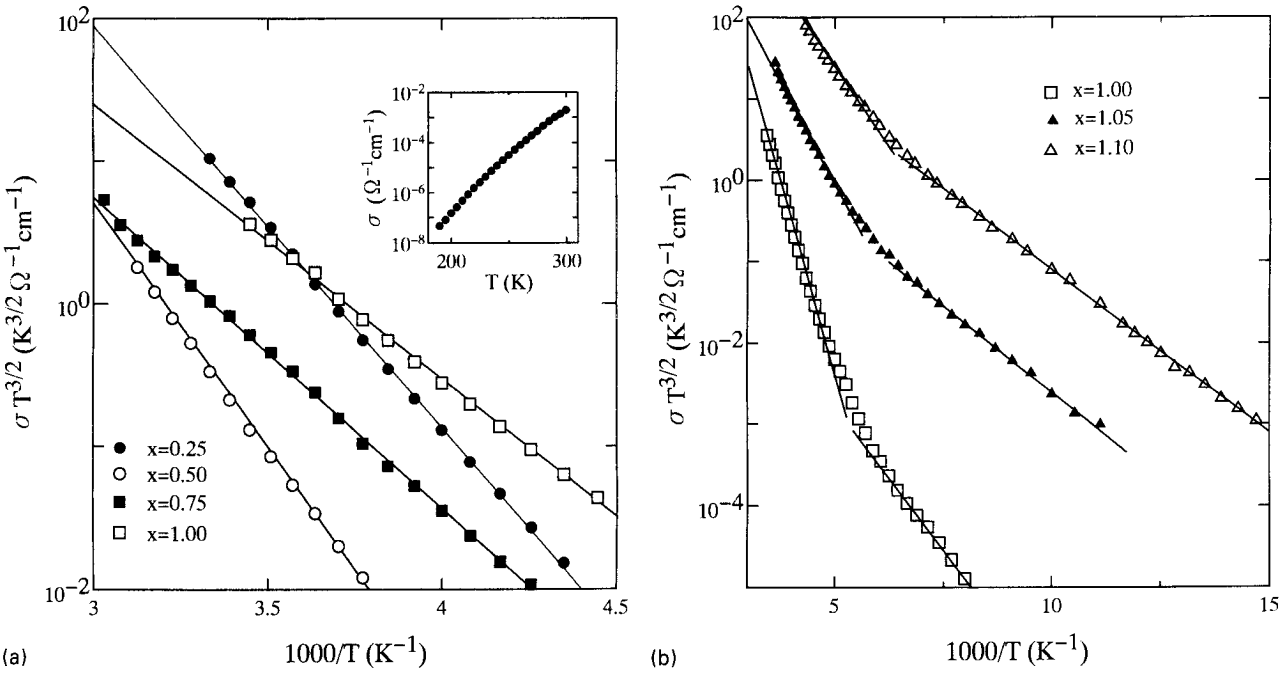

FIG. 3. Arrhenius relations of $\sigma \cdot T^{3/2}$ vs $1/T$ for (a) $x = 0.25, 0.50, 0.75$, and 1.00 at $T > 220$ K and (b) $x = 1.00, 1.05$, and 1.10 at $T > 70$ K, where σ is the bulk conductivity. Solid lines represent thermally activated conduction processes; there are two conduction processes in each specimen for $x \geq 1.00$. The inset demonstrates the relationship between σ and T for $x = 0.25$.

In every specimen, a relaxation process appears in dielectric loss tangent ($\tan\delta$) and electric modulus (imaginary part, M''). Figure 4 plots realistic loss tangent and electric modulus as a function of applied frequency at several temperatures for $x = 1.05$ as an example. The realistic dielectric loss tangent values are obtained by subtracting low-frequency contributions in a method similar to Lalevic *et al.* (39). In each specimen of $x = 1.05$ and 1.10, it should

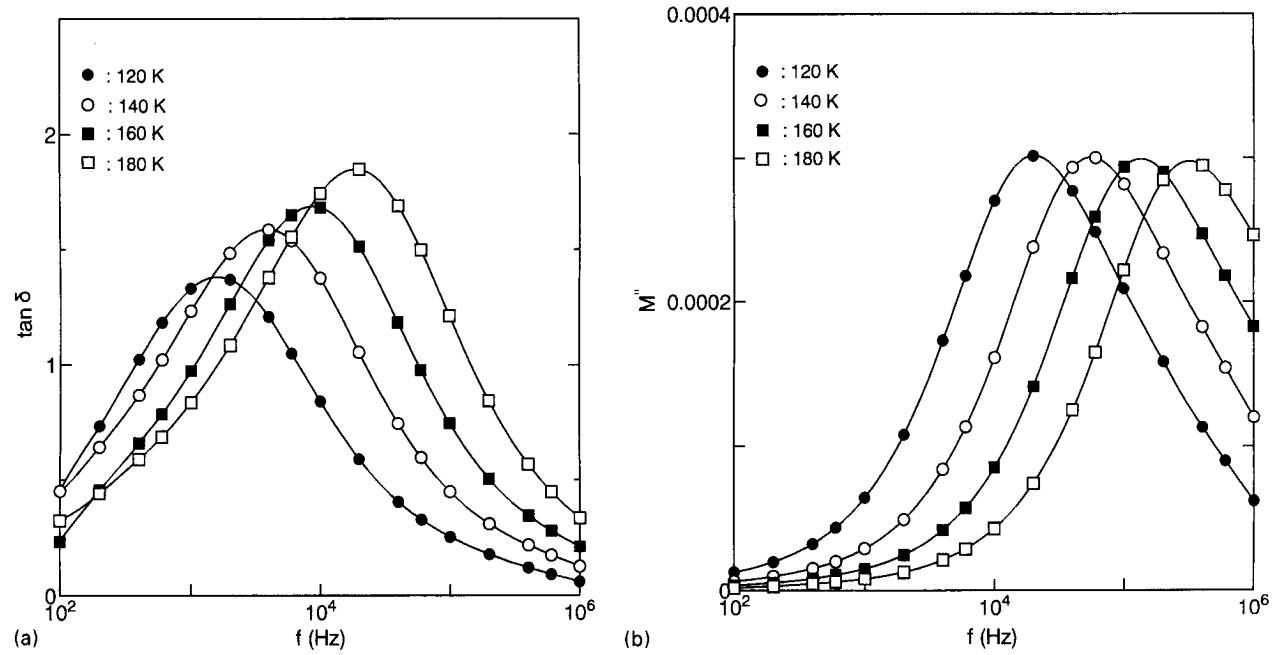

FIG. 4. (a) Frequency dependencies of loss tangent, $\tan\delta$, and (b) electric modulus, M'', at 120, 140, 160, and 180 K for $x = 1.05$.

be noted that the dielectric relaxation occurs in the ferromagnetic regime below the Curie point, where the low-temperature, thermally activated process governs conduction. A dielectric relaxation process corresponding to the high-temperature, thermally activated conduction process in these specimens requires frequencies much higher than the maximum in the present study.

DISCUSSION

The bulk conductivities plotted in Fig. 3 seem surely to favor the polaronic scenario in the electrical transports of the $La_{2-x}Sr_xCoO_4$ system, as suggested in previous reports (10–12). The Arrhenius relation in Fig. 3 represents the nonadiabatic scheme, but this analysis requires more direct evidence, which is available in the dielectric results of Fig. 4.

The dielectric behavior in the $La_{2-x}Sr_xCoO_4$ system is described approximately by Debye's theory (40, 41). At a temperature T, then, the loss tangent and the electric modulus have maxima at the resonance frequencies, $f_{\tan\delta}$ and f_M, respectively, i.e., $(\tan\delta)_{\max} = (\varepsilon_0 - \varepsilon_\infty)/2\sqrt{\varepsilon_0\varepsilon_\infty}$ at $f_{\tan\delta} = \sqrt{\varepsilon_0/\varepsilon_\infty}/2\pi\tau$ and $M_{\max} = (\varepsilon_0 - \varepsilon_\infty)/2(\varepsilon_0\varepsilon_\infty)$ at $f_M = (\varepsilon_0/\varepsilon_\infty)/2\pi\tau$, where ε_0 and ε_∞ are the static and high-frequency dielectric constant, and τ is the relaxation time at T, which has a form of $\tau = \tau_0 \exp(Q/k_BT)$, Q being the activation energy required for the dielectric relaxation. In the polaronic scenario (17–21), the activation energy is the hopping energy, i.e., $Q = W_H$. In the nonadiabatic case, $\tau_0 = 2\hbar(W_H k_B T)^{1/2}/\pi^{1/2}J^2$, where J is the electron transfer integral between neighboring hopping sites and $\hbar$ is Planck's constant divided by 2π (42, 43).

Using the frequencies yielding the maxima of the loss tangent and electric modulus, one has the relation $(f_{\tan\delta})^2 T^{1/2}/f_M = [J^2/4\pi^{1/2}\hbar(W_H k_B)^{1/2}] \exp(-W_H/k_BT)$. For $x \leq 1.00$, Fig. 5a plots the Arrhenius relations of $(f_{\tan\delta})^2 T^{1/2}/f_M$ and $1/T$ at $T > 220$ K, which yield $W_H =$ 0.47, 0.58, 0.41, and 0.35 eV and $J = 0.004$, 0.016, 0.0009, and 0.0008 eV for the specimens $x = 0.25$, 0.50, 0.75, and 1.00, respectively. According to Holstein and Emin (42, 43), nonadiabatic small polaron conduction demands the following two conditions for the electron transfer integral J; $J < 4W_H$; and $J < (W_H k_B T)^{1/4}(\hbar\omega_{OL})^{1/2}$, where ω_{OL} is the frequency of the longitudinal optical mode. The frequency values of the $La_{2-x}Sr_xCoO_4$ system are not yet available but experimental values for similar materials lie in the range 10^{13}–10^{14} s^{-1} (44, 45). The first condition holds in these specimens because $J < W_H$. Employing $\omega_{OL} \cong 10^{13}$ s^{-1} and $T \cong 220$ K, the magnitudes of $(W_H k_B T)^{1/4}(\hbar\omega_{OL})^{1/2}$ are calculated to be 0.018, 0.019, 0.018, and 0.017 eV for $x = 0.25$, 0.50, 0.75, and 1.00, which are larger than J values in these specimens. This assessment definitely meets the requirements for nonadiabatic hopping conduction. Consequently the nonadiabatic Arrhenius plots in Fig. 3a are justified. Furthermore, the electrical transport of large polarons is excluded in this system because the carrier mobility, which is proportional to $\exp(-W_H/k_BT)$, increases with increasing temperature.

The activation energy required for conduction due to a hopping process of small polarons is the sum of the hopping energy, W_H, and half of the potential difference between a free polaron and a polaron bound to a trap, W_O, i.e., $E = W_H + W_O/2$ (17–21). Disordered energy is omitted here because it is generally negligibly small in crystalline bulks compared with W_H, even less than the experimental error in the determination of W_H (46). The hopping energies for $x = 0.25$, 0.50, 0.75, and 1.00 have already been obtained using the frequencies, $f_{\tan\delta}$ and f_M, as shown in Fig. 5a. There is another dielectric relation which yields the value for W_O, i.e., $(\tan\delta)^2_{\max} T/M''_{\max} \propto \exp(-W_O/2k_BT)$ (18–21). As shown in Fig. 6a, the straight lines in Arrhenius relations of $(\tan\delta)^2_{\max} T/M''_{\max}$ and $1/T$ yield $W_O/2 = 0.11$, 0.09, 0.03, and 0.03 eV for $x = 0.25$, 0.50, 0.75, and 1.00, respectively. The sum of the energies obtained independently in Figs. 5a and 6a is very close to the activation energy in Fig. 3a for every specimen of $x \leq 1.0$.

With increasing x from 0.25 to 0.50, the conductivities decrease remarkably, whereas the conductivities increase as x increases from 0.50 as shown in Fig. 3a. In the layered-type perovskite oxides, a charge- and spin-ordered state is frequently observed when the carrier concentration takes a commensurate value (e.g., $x = 1/8$, 1/3, or 1/2) (51–54). In the $La_{2-x}Sr_xCoO_4$ system, the specimen of $x = 0.50$ has the lowest conductivities and the maximum hopping energy in the temperature region where the impedance analyses are possible. This feature agrees with the result of Morimoto *et al.* (32). The ordered state results in a deep polaron state of holes, that is, the polaron binding energy, W_P, takes the maximum value. Since the hopping energy is related to the binding energy as $W_H = W_P/2 - t'$ where t' is a quantity less than the band width (13), the hopping energy in the ordered state is also expected to take the maximum value. The peculiarity at $x = 0.50$ observed in this system might be due to the commensurability of x with the lattice periodicity and resultant real space ordering of the doped holes. This speculation coincides well with the magnetic analysis of Morimoto *et al.* (32).

There must be several reasons for the increment in conductivity with x increasing from 0.50. In the spin-state transition study by Morimoto *et al.* (32), the Co^{3+} and Co^{2+} ions are in the HS state for $x \leq 0.60$, in the IS state for $0.80 \leq x \leq 1.00$, and the transition from the HS state to the IS state occurs for $0.60 \leq x \leq 0.80$. In the HS state, the nonadiabatic small polaron of a hole hops from Co^{3+} to Co^{2+} ions via a t_{2g} level in the upper Hubbard band (32). In the IS state, Morimoto *et al.* (32) consider the transfer of e_g electron of the neighbouring Co^{ii} to Co^{iii} and argue that the itinerant e_g electrons (and/or holes) can mediate

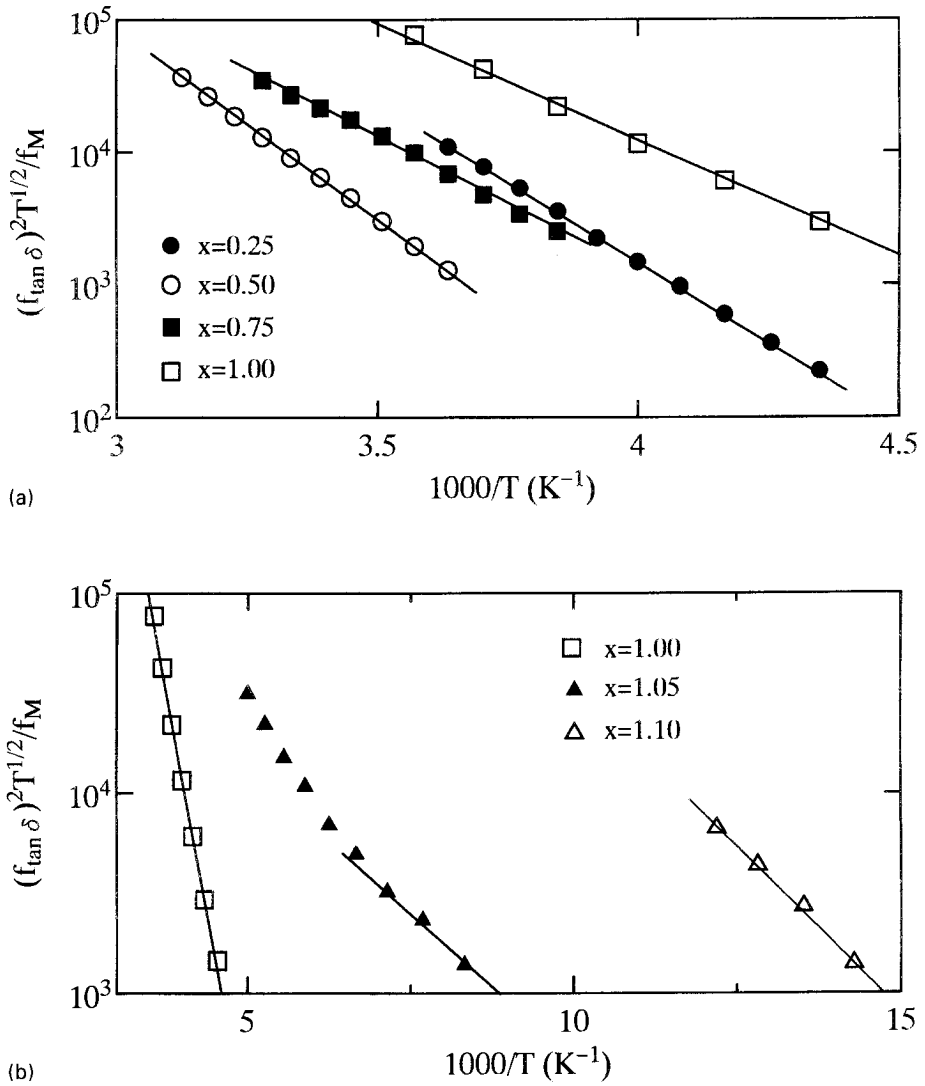

FIG. 5. Arrhenius relations between $(f_{\tan\delta})^2T^{1/2}/f_M$ and $1/T$ for (a) $x = 0.25$, 0.50, 0.75, and 1.00 and (b) $x = 1.00$, 1.05, and 1.10.

a ferromagnetic interaction between the neighbouring Co spins, analogous to the double-exchange mechanism (51). The itinerant carriers enhance the electrical conduction and consequently the conductivity increases as the amount of itinerant carriers increases. In the present study, however, the carriers are still localized even in the specimens with $x \geq 0.75$ because these specimens undergo dielectric relaxation due to a hopping process of carriers, as shown in Fig. 4, but the reduction of the hopping energy with increasing x indicates that the carriers become more itinerant. Referring to the positive Seebeck coefficients in the $La_{2-x}Sr_xCoO_4$ system (11), the hopping process of the nonadiabatic small polarons of holes via an e_g level in the lower Hubbard band must be predominantly responsible for the electrical transports below room temperature for $0.75 \leq x \leq 1.00$.

Mobile nonadiabatic small polarons, i.e., free polarons, are created by releasing holes trapped at imperfections by W_O, which is the potential difference between a free polaron and a polaron bound to a trap. Just like $La_{1-x}Sr_xCoO_3$ (52), Sr^{2+} ions must play a somewhat important role in the formation of traps. With increasing x, W_O decreases as shown in Fig. 6a. Such a behavior could be explained by the speculation that an increase in the repulsive Coulombic interaction between Sr^{2+} ions with increasing x increases the potential level of the polaron bound to a trap, reducing the potential difference.

For $x \geq 1.00$, the conduction feature differs considerably from that in Fig. 3a. Even the specimen $x = 1.00$ contains a low-temperature conduction process, as do the specimens $x = 1.05$ and 1.10. Though there is no legitimate reason to employ the nonadiabatic Arrhenius plots for $x = 1.05$ and

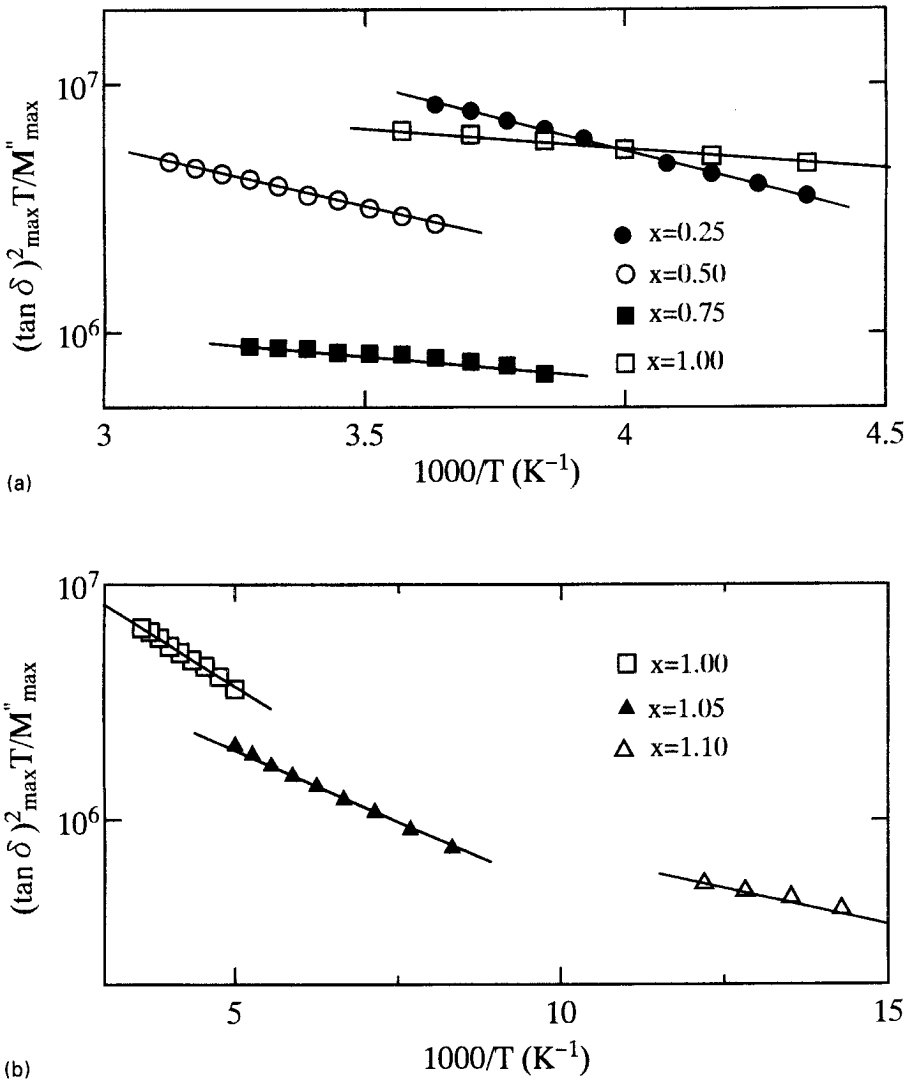

FIG. 6. Arrhenius relations between $(\tan\delta)^2_{max}T/M''_{max}$ and $1/T$ for (a) $x = 0.25$, 0.50, 0.75, and 1.00 and (b) $x = 1.00$, 1.05, and 1.10.

1.10, Figure 3b follows the illustration in Fig. 3a for the sake of convenience. The activation energies in the low-temperature processes of these specimens are remarkably small compared with those in the high-temperature processes. These energies do not differ so much even if adiabatic Arrhenius plots are used. The low-temperature conduction takes place in the ferromagnetic regimes of these specimens below Curie points (~220 K–~200 K) (31). Since the dielectric relaxation processes in the specimens $x = 1.05$ and 1.10 also show up below Curie points, as shown in Figs. 4a and 4b, J values in the high-temperature conduction processes of these specimens are impossible to estimate using the dielectric relaxations observed in the present study.

The Arrhenius relations of $(f_{\tan\delta})^2T^{1/2}/f_M$ and $1/T$ are demonstrated in Fig. 5b for the specimens $x = 1.00$, 1.05, and 1.10. The specimen $x = 1.05$ contains the transition from the high-temperature process to the lower-temperature one; the transition point and the conduction result are near the Curie temperature. There are, however, only straight lines for $x = 1.00$ and 1.10. The temperature region in which the dielectric relaxation is observable in loss tangent and electric modulus is very narrow in comparison with the temperature region where the impedance analyses are possible. Then, the plots in Fig. 5b for $x = 1.00$ correspond to the high-temperature conduction process, as discussed above, while the plots for $x = 1.10$ are within the temperature region of the low-temperature conduction process. In fact, the activation energy for $x = 1.10$ in Fig. 5b is 0.065 eV, which is very close to the energy required for the low-temperature conduction process, i.e., 0.079 eV. As for the specimen $x = 1.05$, the activation energy in the low-temperature process is estimated to be 0.064 eV, which is

also competitive with the activation energy required for the low-temperature conduction process, i.e., 0.083 eV. Furthermore, the energies required for the dielectric relaxations in the ferromagnetic phases $x = 1.05$ and 1.10 are practically the same.

Figure 6b demonstrates the Arrhenius relations of $(\tan\delta)^2_{max}T/M''_{max}$ and $1/T$ for $x = 1.00$, 1.05, and 1.10. All specimens have straight lines with $W_O/2 = 0.036$, 0.025, and 0.013 eV for $x = 1.00$, 1.05, and 1.10, respectively, and there is no transition even in the specimen $x = 1.05$. The sum of W_H and $W_O/2$ is nearly equal to the activation energy required for the bulk conduction in the ferromagnetic phase for $x = 1.05$ and 1.10. The feature in Fig. 5b is surely indicative of the strong correlation between local spin alignment and the hopping process of carriers in the ferromagnetic phase. But the result in Fig. 6b suggests that local spin alignment scarcely influences the polaron binding energy, W_P, in the ferromagnetic phase; instead the long-range Coulombic interaction looks rather important.

Though the present study unfortunately cannot elucidate the real future of the carriers in the ferromagnetic $La_{2-x}Sr_xCoO_4$ phase at low temperatures, the study on the spin-state transition in $La_{1-x}Sr_xCoO_3$ by Yamaguchi *et al.* (53) provides significant suggestions on this issue. When even a very slight amount of Sr ions, i.e., $x = 0.002$, is doped into $LaCoO_3$, the susceptibility drop due to the high-to-low spin-state transition with decreasing temperature is suppressed and instead a Curie-like contribution is remarkably increased. Then an extended wave function of a $2p$ doped-hole is expected to form a spin polaron whereas the hopping process of adiabatic small polarons dominates the electrical transport in nondoped $LaCoO_3$ (20). Mott and Davis (54) do not think that spin polaron formation can give rise to hopping motion in a perfect crystal. This must be mainly because spin-gap values are generally very small and thus undetectable experimentally. Emin *et al.* argue, however, that the intra-atomic exchange due to spin-spin interactions, in tandem with the very short component of the electron-phonon interaction, localize carriers in ferromagnets (55, 56). Then, a hopping process of spin polarons could be observable experimentally in ferromagnets, but with a rather low activation energy. In fact, the spin polaron picture is indicative of an extremely low activation energy for a hopping process of spin polarons (55–59). Though speculation like this indicates the possibility that spin polarons could be the majority carrier in the ferromagnetic phase of $La_{2-x}Sr_xCoO_4$, more direct experimental evidence is required.

CONCLUSION

Electrical transports in the $La_{2-x}Sr_xCoO_4$ system ($x = 0.25$, 0.50, 0.75, 1.00, 1.05, and 1.10) below room temperature were investigated by bulk conductivities and dielectric properties in polycrystalline specimens. The bulk conductivities were obtained by complexplane impedance analyses. The positive Seebeck coefficients in the $La_{2-x}Sr_xCoO_4$ system indicate that the doped holes are the majority carrier. For $x \leq 1.00$, every specimen contains a dielectric relaxation process in loss tangent and electric modulus. The relative relation of the frequencies yielding the maxima of the loss tangent and modulus yield the hopping energy, W_H, and the electron transfer integral between neighbouring hopping sites, J. These energies in every specimen meet the requirements for nonadiabatic hopping conduction. Another dielectric relation between the maxima of the loss tangent and modulus also provides the magnitude for the potential difference between a free polaron and a polaron bound to a trap, W_O. The activation energy obtained in the Arrhenius relation $\sigma \cdot T^{3/2}$ and $1/T$ at $T > 220$ K is nearly equal to the sum of W_H and $W_O/2$. These results indicate that the electrical transports for $x \leq 1.00$ are described in terms of a hopping process of nonadiabatic small polarons of holes at $T > 220$ K. A peculiarity due to the charge- and spin-ordered state is observed in the conduction behaviour at $x = 0.5$.

For $x \geq 1.00$, every specimen involves the transition from the high-temperature thermally activated conduction process to the low-temperature one. The transition temperature corresponds well to the Curie point. Thus the low-temperature conduction takes place in the ferromagnetic phase. There is also a transition in the relationship of the frequencies yielding the maxima of the loss tangent and modulus for $x = 1.05$. As for $x = 1.00$ and 1.10, there are only straight lines, because the dielectric relaxation in the loss tangent and the modulus appears in the high-temperature conduction region for $x = 1.00$ and in the low-temperature conduction region for $x = 1.10$. These results indicate the strong correlation between local spin alignment and the hopping process of carriers in the ferromagnetic phase. Though the possibility that a spin polaron is the majority carrier in the ferromagnetic phase is speculated, more direct experimental evidence is required.

ACKNOWLEDGMENTS

The authors are very grateful to N. Nakamura, W. H. Jung, K. Ueda, and E. Akima for useful discussion and assistance in this project. This project was supported by a Grant-in-Aid for Science Research (08650812) from the Ministry of Education, Science and Culture, Japan, and Takahashi Industrial and Economic Foundation.

REFERENCES

1. G. Bednorz and K. A. Müller, *Z. Phys. B* **64,** 189 (1986).
2. D. Emin, *Phys. Rev. Lett.* **62,** 1544 (1989).
3. D. Emin, *Phys. Rev. B* **45,** 5525 (1992).
4. D. Emin, *Phys. Rev. B* **48,** 13691 (1993).
5. P. Ganguly and S. Ramasesha, *Magnetism Lett.* **1,** 131 (1980).

6. G. Demazeau, P. Courbin, G. Le Flem, M. Pouchard, P. Hagenmuller, J. L. Soubeyroux, I. G. Main, and G. A. Robins, *Nouv. J. Chim.* **3,** 171, (1979).
7. G. Demazeau, P. Courbin, I. G. Main, and G. Le Flem, *C. R. Acad. Sci. Ser. C* **283,** 61 (1976).
8. G. Blasse, *J. Inorg. Nucl. Chem.* **27,** 2683 (1965).
9. J. J. Janecek and G. P. Wirtz, *J. Am. Ceram. Soc.* **61,** 242 (1978).
10. L. R. Le Coustumer, Y. Barbaux, and J. P. Bonnelle, *Nouv. J. Chim.* **6,** 7 (1982).
11. T. Matsuura, J. Tabuchi, J. Mizusaki, S. Yamauchi, and K. Fueki, *J. Phys. Chem. Solids* **49,** 1403 (1988).
12. T. Matsuura, J. Tabuchi, J. Mizusaki, S. Yamauchi, and K. Fueki, *J. Phys. Chem. Solids* **49,** 1409 (1988).
13. I. G. Austin and N. F. Mott, *Adv. Phys.* **18,** 41 (1969).
14. R. Gehlig and E. Salje, *Philos. Mag. B* **47,** 229 (1983).
15. A. Mansingh, J. M. Reyes, and M. Sayer, *J. Non-Cryst. Solids* **7,** 12 (1972).
16. H. A. A. Sidek, I. T. Collier, R. N. Hampton, G. A. Sauders, and B. Bridge, *Philos. Mag. B* **59,** 221 (1989).
17. E. Iguchi and K. Akashi, *J. Phys. Soc. Jpn.* **61,** 3385 (1992).
18. W. H. Jung and E. Iguchi, *Philos. Mag. B* **73,** 873 (1996).
19. E. Iguchi, T. Hashimoto, and S. Yokoyama, *J. Phys. Soc. Jpn.* **65,** 221 (1996).
20. E. Iguchi, K. Ueda, and W. H. Jung, *Phys. Rev. B* **54,** 17431 (1997).
21. E. Iguchi and N. Nakamura, *J. Phys. Chem. Solids* **58,** 755 (1997).
22. T. Holstein, *Annals Phys.* **8,** 343 (1959).
23. D. Emin, *Phys. Rev. B* **4,** 3639 (1971).
24. M. A. Kolber and R. K. MacCrone, *Phys. Rev. Lett.* **29,** 1457 (1972).
25. F. G. Koffyberg and F. A. Benko, *J. Non-Cryst. Solids* **40,** 7 (1980).
26. G. Le Flem, G. Demazeau, and P. Hagenmuller, *J. Solid State. Chem.* **44,** 82 (1982).
27. M. Seppanen and M. H. Tikkanen, *Acta Chem. Scand.* **30,** 389 (1976).
28. A. Rabenau and P. Eckerlin, *Acta Crystallogr.* **11,** 304 (1958).
29. U. Lehmann and H. K. Muller-Buschbaum, *Z. Anorg. Allg. Chem.* **470,** 59 (1980).
30. G. Payom and M. Daire, *Rev. Chim. Minerale* **14,** 11 (1977).
31. Y. Furukawa, S. Wada, and Y. Yamada, *J. Phys. Soc. Jpn.* **62,** 1127 (1993).
32. Y. Morimoto, K. Higashi, K. Matsuda, and A. Nakamura, *Phys. Rev. B* **55,** R14725 (1997).
33. J. Zaanen, G. A. Sawatzky, and J. W. Allen, *Phys. Rev. Lett.* **55,** 418 (1986).
34. Y. Morimoto, T. Arima, and Y. Tokura, *J. Phys. Soc. Jpn.* **64,** 4117 (1995).
35. G. Demazeau, B. Bernard, M. Pouchard, and P. Hagenmuller, *J. Solid State Chem.* **54,** 389 (1984).
36. J. R. MacDonald, *J. Chem. Phys.* **61,** 3977 (1974).
37. J. R. MacDonald, *in* "Superionic Conductors," p. 1. Plenum, New York, 1976.
38. A. D. Franklin, *J. Amer. Ceram. Soc.* **58,** 465 (1975).
39. B. Lalevic, N. Fuschillo, B. Kuliyev, and W. Wang, *Appl. Phys.* **5,** 127 (1974).
40. H. Frölich, *in* "Theory of dielectrics," p. 70. Oxford, Clarendon, 1958.
41. R. Gehardt, *J. Phys. Chem. Solids* **55,** 1491 (1994).
42. T. Holstein, *Annals Phys.* **8,** 343 (1959).
43. D. Emin, *Phys. Rev. B* **4,** 3639 (1971).
44. J. C. Phillips, *in* "Physics of High-Tc Superconductors," Chapter 4. Academic Press, San Diego, 1989.
45. R. Raffaelle, H. U. Anderson, C. D. Sparlin, and D. Parris, *Phys. Rev. B* **43,** 7991 (1991).
46. L. A. K. Dominik and R. K. MacCrone, *Phys. Rev.* **163,** 756 (1967).
47. J. M. Tranquada, B. J. Sternlieb, J. D. Axe, Y. Nakamura, and S. Uchida, *Nature (London)* **337,** 561 (1995).
48. C. H. Chen, S.-W. Cheong, and A. S. Cooper, *Phys. Rev. Lett.* **71,** 2461 (1993).
49. Y. Morimoto, Y. Tomioka, A. Asamitus, and Y. Tokura, *Phys. Rev. B* **51,** 3297 (1995).
50. B. J. Sternlieb, J. P. Hill, C. Wildgruber, G. M. Luke, B. Nachumi, Y. Morimoto, and Y. Tokura, *Phys. Rev. Lett.* **76,** 2169 (1996).
51. P. W. Anderson and H. Hasegawa, *Phys. Rev. B* **100,** 675 (1955).
52. M. A. Señarís-Rodríguez and J. B. Goodenough, *J. Solid State Chem.* **118,** 323 (1995).
53. S. Yamaguchi, K. Okimoto, H. Taniguchi, and Y. Tokura, *Phys. Rev. B* **53,** R2926 (1996).
54. N. F. Mott and E. A. Davis, *in* "Electronic Processes in Non-Crystalline Materials," 2nd ed., p. 156. Oxford Univ. Press, Oxford, 1979.
55. D. Emin, M. S. Hilley, and N. H. Liu, *Phys. Rev. B* **33,** 2933 (1986).
56. D. Emin, M. S. Hilley, and N. H. Liu, *Phys. Rev. B* **35,** 641 (1986).
57. S. von Malnar and S. Methfessel, *J. Appl. Phys.* **38,** 953 (1967).
58. T. Kasuya, A. Yanase, and T. Taketa, *Solid St. Commun.* **8,** 1551 (1970).
59. J. Blasco and J. Carcía, *J. Phys.: Condens. Matter* **6,** 10759 (1994).